Published in final edited form as:
*Mol Cell*. 2013 November 7; 52(3): 325–339. doi:10.1016/j.molcel.2013.08.043.

# Metabolic activation of CaMKII by Coenzyme A

**Francis McCoy**[1], **Rashid Darbandi**[1], **Hoi Chang Lee**[8], **Kavitha Bharatham**[2], **Tudor Moldoveanu**[3], **Grace Royappa**[4], **Keela Dodd**[1], **Wenwei Lin**[2], **Si-Ing Chen**[1], **Rajendra P Tangallapally**[2], **Manabu Kurokawa**[5], **Richard E. Lee**[2], **Anang Shelat**[2], **Taosheng Chen**[2], **Douglas R. Green**[3], **Robert A. Harris**[6], **Sue-Hwa Lin**[7], **Rafael A. Fissore**[8], **Roger J. Colbran**[9], and **Leta K. Nutt**[1,#]

[1]Department of Biochemistry, St. Jude Children's Research Hospital, 262 Danny Thomas Place, Memphis, TN 38105

[2]Department of Chemical Biology, St. Jude Children's Research Hospital, 262 Danny Thomas Place, Memphis, TN 38105

[3]Department of Immunology, St. Jude Children's Research Hospital, 262 Danny Thomas Place, Memphis, TN 38105

[4]Department of Structural Biology, St. Jude Children's Research Hospital, 262 Danny Thomas Place, Memphis, TN 38105

[5]Department of Pharmacology and Toxicology, Geisel School of Medicine, Dartmouth College, Hanover, NH 03755

[6]Department of Biochemistry and Molecular Biology, Indiana University School of Medicine, Indianapolis, IN 46202

[7]Department of Translational Molecular Pathology, The University of Texas MD, Anderson Cancer Center, Houston, TX 77030

[8]Department of Veterinary and Animal Sciences, University of Massachusetts, Amherst, MA 01003

[9]Department of Molecular Physiology and Biophysics, Vanderbilt Brain Institute and Kennedy Center for Research on Human Development, Vanderbilt University School of Medicine, Nashville, TN 37232

## SUMMARY

Active metabolism regulates oocyte cell death via calcium/calmodulin-dependent protein kinase II (CaMKII) mediated phosphorylation of caspase-2, but the link between metabolic activity and CaMKII is poorly understood. Here we identify coenzyme A (CoA) as the key metabolic signal that inhibits *Xenopus laevis* oocyte apoptosis, in a novel mechanism of CaMKII activation. We found that CoA directly binds to the CaMKII regulatory domain in the absence of $Ca^{2+}$ to activate CaMKII in a calmodulin-dependent manner. Furthermore, we show that CoA inhibits apoptosis not only in *X. laevis* oocytes, but also in *Murine* oocytes. These findings uncover a novel



[#]To whom correspondence should be addressed: Leta Nutt, PhD, Assistant Member, Department of Biochemistry, MS 340, St. Jude Children's Research Hospital, 262 Danny Thomas Place, Memphis, TN 38105, Tel.: Office: 901-595-6530; Lab: 901-595-2030; Fax: 901-525-8025; leta.nutt@stjude.org.

mechanism of CaMKII regulation by metabolism and further highlight the importance of metabolism in preserving oocyte viability.

## INTRODUCTION

The dogma that primary oocytes formed at birth are a nonrenewable source of eggs was challenged by the discovery of proliferative germ cells that sustain oocyte and follicle production(Johnson et al. 2004). Nevertheless, the number of mature oocytes that eventually ovulate as an egg over the menstrual lifespan of a woman remains fixed at approximately 400 (Gosden 2005). Age-related aneuploidy, chemotherapy treatment, or environmental toxin insult causes death, or atresia, of vertebrate oocytes, which in turn leads to premature menopause and infertility. Because the first birthrates for women aged 35–44 years have increased eightfold, there is a renewed interest in developing oocyte-preserving strategies.

One way to prevent oocyte atresia is by inhibiting specific proteins in the cell death pathway (Gosden 2005); Lobo 2005). The first evidence that dormant female germ cells possess the machinery for programmed cell death was the demonstration of doxorubicin-induced apoptosis in vertebrate oocytes (Perez et al. 1997). We also reported that nutrient deprivation induces apoptosis of vertebrate oocytes via activation of caspase-2(Nutt et al. 2005;Nutt et al. 2009). This is particularly interesting because the primary phenotype of caspase-2 knockout mice is excess accumulation of oocytes that are resistant to doxorubicin-induced cell death, suggesting that vertebrate oocytes are particularly susceptible to caspase-2–mediated death (Bergeron et al. 1998). While exploring the links between metabolism and caspase-2, we discovered that the addition of NADPH/glucose 6-phosphate (G6P) to oocyte extracts generates an unidentified metabolic factor which suppresses the initiation of the apoptotic signaling cascade by activating calcium/calmodulin-dependent protein kinase II (CaMKII) (Nutt et al. 2005). CaMKII activation by NADPH/G6P was independent of an increase in cytosolic $Ca^{2+}$, suggesting the involvement of a novel non-canonical pathway.

The four CaMKII isoforms (α, β, γ, and δ) form a family of multifunctional serine/threonine protein kinases that are important in many signaling cascades ranging from learning and memory to the exit from mitosis. CaMKII exists as a homo-or hetero-dodecamer (Hudmon & Schulman 2002). $Ca^{2+}$/calmodulin (CAM)-stimulated autophosphorylation at Thr-286/287 - the canonical CaMKII activation pathway - results in formation of a constitutively active form of CaMKII that is essential for normal signaling. Targeted, isoform-specific deletion of CaMKII results in very specific and diverse phenotypes in mice, but CaMKIIγ−/− mice are uniquely infertile because of egg-activation defects(Backs et al. 2010). The biochemistry detailing the requirement for CaMKII in egg activation was first demonstrated using the *Xenopus* egg. Our previous data further demonstrate that in *X. laevis* oocytes CaMKII is a hetero-dodecamer, composed of multiple isoforms (McCoy et al. 2013).

Although genetic analyses in mice have improved our understanding of vertebrate infertility, most vertebrate oocytes are not amenable to biochemical analysis due to their small size and limited abundance. To identify the NADPH/G6P–dependent factor(s) required for CaMKII activation, we used the biochemically tractable *X. laevis* egg extract and oocyte in this study. Using cellular fractionation and unbiased metabolomics, we showed that addition of G6P to *X. laevis* egg extracts preserved and increased cytosolic free CoA levels. We found that free CoA directly binds to the calmodulin binding domain(CAMBD) of CaMKII to promote CAM binding and activation of CaMKII in the absence of any increase in $Ca^{2+}$. CaMKII then phosphorylates caspase-2 at Ser135 and promotes oocyte survival. This is the first evidence of CoA directly regulating CaMKII and oocyte survival. Furthermore, we provide

strong evidence that this unique metabolic regulation of oocyte survival is evolutionarily conserved in mammalian oocytes.

## RESULTS

### G6P-Induced CaMKII Activation Requires a Heat-Soluble Cytosolic Factor

Our earlier study showed that addition of G6P to *X. laevis* egg extracts increases NADPH levels and suppresses oocyte death via CaMKII activation (Nutt et al. 2005). To test whether NADPH directly activates CaMKII to suppress caspase-2 activation, NADPH was incubated with recombinant CaMKIIα and CAM. As shown in Fig. 1A, addition of NADPH to CaMKIIα and CAM did not activate CaMKIIα to phosphorylate caspase-2 at S135, unlike $Ca^{2+}$. This indicates that NADPH does not directly activate CaMKII to suppress apoptosis.

As a first step toward identification of G6P/NADPH–dependent factor(s) required for CaMKII activation and the inhibition of apoptosis, G6P-treated and untreated egg extracts were biochemically fractionated using a combination of heat precipitation and affinity chromatography (Fig. 1B). CaMKIIα was added to heat soluble cytosolic fractions, and CaMKII activity was determined by substrate phosphorylation of caspase-2 at S135. The G6P-dependent factor(s) responsible for CaMKII activation was heat stable (Fig. 1C).

CAM is a well-known heat-stable activator of CaMKII. In order to determine the contribution of CAM to CaMKII activation by the heat-soluble cytosolic fractions, we first depleted CAM from the samples using a CAM-binding domain (CAMBD) peptide, amino acids 290–309 of CaMKII, coupled to Sepharose. Depletion using CAMBD-Sepharose markedly inhibited the activation of CaMKIIα, even when samples were supplemented with CAM (Fig. 1D). These observations suggest that CAMBD-Sepharose may have depleted not only CAM, but also other factors, from the heat-soluble fraction that may be involved in CaMKII activation. Consistent with this idea, depletion of CAM using phenyl-Sepharose, a hydrophobic resin classically used to purify CAM, also prevented CaMKII activation, but in this case activation was restored by addition of CAM (Fig. 1D). However, serial depletion of extracts, first by phenyl-Sepharose (to remove CAM) and then subsequently by CAMBD-Sepharose, removed the metabolic factor required for CAM-dependent CaMKII activation (Fig. 1D). In combination, these findings suggest that the heat-soluble cytosolic fraction of *X. laevis* egg extracts contains two factors that are important for CaMKII activation; CAM, which can be depleted by phenyl-Sepharose or CAMBD-Sepharose, in addition to another heat-stable factor that is only depleted using CAMBD-Sepharose.

### G6P Increases the Level of Cytosolic Coenzyme A

Initial proteomics-based efforts to identify the G6P-induced heat-soluble factor that contributed to CaMKII activation were unsuccessful. Therefore, we used an unbiased metabolomics approach to follow carbon flow in *X. laevis* egg extracts prior to (0 and 3 hours), and following (4 hours), caspase activation +/− G6P. Extracts were subjected to high-speed centrifugation to remove light and heavy membranes, and cytosolic extracts were analyzed. As expected, the levels of glucose, G6P, and glycolytic intermediates were substantially higher in G6P-treated extracts compared to control extracts. Levels of glucose-1-phosphate were also higher, perhaps implying an increase in glycogenesis which has already been established in the *X. laevis* egg and oocyte (Nutt 2012). Intermediates of the pentose phosphate pathway were also higher following G6P addition (Fig. S1&2). We detected a significant increase in total levels of acetyl CoA in the G6Ptreated extracts (Fig. 2A). Moreover, adding acetyl CoA to egg extracts activated CaMKII as assessed by caspase-2 phosphorylation and anti-T286/7 phospho-CaMKII immunoblot (Fig. 2B and C),

and inhibited the activation of caspase-3 and caspase-2, similar to the effects of G6P (Fig. 2D and E).

Increased levels of cytosolic acetyl CoA have been detected in cancer (Wellen et al. 2009) and can modify protein activity by acetylation. Although increased cytosolic acetyl CoA by G6P increased global acetylation in the extract, we found no evidence that protein acetylation was involved. Neither recombinant caspase-2 nor CaMKII were acetylated in the presence of G6P, as assessed by immunoblotting with an acetyl-lysine antibody (data not shown). Furthermore, mass spectrometric analysis for acetylation of CaMKII was negative for total acetylation (data not shown). These observations suggest that G6P increases the level of cytosolic acetyl CoA, which signals CaMKII activation in an acetylation-independent manner. In order to define functional regions in the acetyl CoA structure, we compared caspase-2 phosphorylation and caspase-3 activation following the addition of CoA, acetyl CoA or acetate to extracts. CoA alone was sufficient to induce phosphorylation of caspase-2 and suppress caspase-3 activation (Fig. 2F and G).

Chemical ablation of the rate-limiting enzyme required for CoA synthesis, panthothenate kinase, did not override G6P-induced mediated inhibition of caspase activation or CaMKII activation (Fig. 2H and I). The fact that CoA alone was sufficient to activate CaMKII and inhibit apoptosis (Fig. 2F and G), and that acyl-CoA hydrolases/thioesterases are highly active *in vivo* (Berge & Farstad 1979b; Knudsen et al. 1999) ,we then hypothesized that acetyl CoA breakdown into CoA was the metabolic signal activating CaMKII. To test whether the addition of G6P-induced an increase in acetyl CoA that may in turn be hydrolyzed to produce cytosolic CoA, we performed LC/MS/MS analysis on heat soluble cytosolic fractions of G6P and acetyl CoA treated extracts, measuring the levels of acetyl CoA and CoA respectively. We found that similar to the result seen Fig. 2A G6P induced a significant ~2.5 fold increase in acetyl CoA levels (Fig. 2J). Furthermore, treatment with acetyl CoA resulted in a substantial increase in CoA levels (Fig. 2K). Taken together these data demonstrate that G6P did not induce a *de novo* synthesis of CoA but rather indirectly increased free CoA levels by increasing acetyl CoA synthesis, which in turn was hydrolyzed to acetate and CoA.

## CoA activates CaMKII and suppresses caspase activation

If CoA were the metabolic signal responsible for activation of CaMKII, then we would predict that caspase activation in control extracts would be preceded by a decrease in levels of CoA. Metabolomic analysis found that after 3 or 4 hrs incubation, the levels of free CoA in control extracts had decreased by approximately 60%, whereas CoA levels in G6P treated extracts had increased by approximately 50%. Thus, prior to caspase activation (4–6 hr in control extracts – see Fig. 2D, F&H), free CoA levels were ~3-fold higher in G6P treated extracts compared to control extracts (Fig. 3A). The correlation of CoA levels, in the absence and presence of G6P, and CaMKII activity suggest that this co-factor may regulate CaMKII and downstream regulation of caspase activation.

To examine whether CoA might play a role in CaMKII activation, CoA was titrated into extracts. CoA increased caspase-2 phosphorylation in a concentration-dependent manner (Fig. 3B), and also enhanced the phosphorylation of endogenous CaMKII at T286/287 (Fig. 3C), similar to G6P. The pattern of the three bands recognized by the phospho-Thr-286/287 antibody is similar to the pattern previously detected using a pan-CaMKII antibody that recognizes the α, β, γ, and δ isoforms of CaMKII (McCoy et al. 2013). Depletion of CaMKII from extracts using CAM-Sepharose inhibited the CoA-dependent phosphorylation of caspase-2 (Fig. 3D), showing that CoAdependent phosphorylation of caspase-2 required CaMKII. Thus, increasing the levels of CoA in egg extracts is sufficient to activate CaMKII. Next we examined whether CoA-dependent CaMKII activation resulted in caspase-2 and

caspase-3 inhibition similar to G6P. CoA supplementation of egg extracts inhibited the activation of caspase-3 and caspase-2, similar to the effects of G6P (Fig. 3E&F). Taken together these data show that maintenance of CoA levels sustains CaMKII activity to suppress caspase activation in egg extracts.

## Coenzyme A (CoA) directly binds endogenous CaMKII

Our biochemical data suggested that a heat-stable factor responsible for CaMKII activation could bind to a CAMBD peptide (Fig. 1). Since CoA is heat-stable and also plays a role in CaMKII activation (Fig. 2&3), we tested the hypothesis that CoA can directly bind to CaMKII. CoA, acetyl CoA, or NADPH were immobilized on Sepharose and incubated with egg extracts. Isolated complexes were analyzed by immunoblotting using the phospho-Thr286/7 specific antibody that detected multiple activated CaMKII isoforms, and a total CaMKII antibody. Fig. 4A shows endogenous CaMKII bound effectively to CoA-Sepharose, while the binding to acetyl CoA-Sepharose was very weak and could only be detected after prolonged film exposure. In contrast, there was no detectable binding to NADPH-Sepharose. This demonstrates that the CoA moiety alone is sufficient to bind CaMKII. To further examine the specificity of this interaction, CaMKII was depleted from extracts using CAM-Sepharose, or mock depleted with Sepharose. These depleted extracts were then incubated with Sepharose or CoA-Sepharose. Proteins recognized by two different antibodies were specifically detected bound to CoA-Sepharose from control extracts, but not from extracts depleted of CaMKII (Fig. 4B). Interestingly, based on the reactivity of the anti-panCaMKII antibody, multiple CaMKII isoforms appeared to interact with CoA-Sepharose. Moreover, binding of CaMKII to CoA-Sepharose was blocked by the prior addition of excess exogenous CoA to the extracts (Fig. 4C). Furthermore, excess exogenous CoA was able to displace CaMKII from an isolated complex with CoA-Sepharose (Fig. 4D). Together, these data establish the specificity of the CoA–CaMKII interaction in egg extracts.

Next, we examined the interaction between a fluorescent CoA derivative (CoA-488) and recombinant His-tagged CaMKIIα, labeled using a terbium (Tb)-conjugated anti-HIS tag antibody (Tb-anti-His), by time-resolved fluorescence resonance energy transfer (TR-FRET) analysis. A CoA-488 concentration-dependent increase in TR-FRET was markedly suppressed by inclusion of excess free CoA (Fig. 4E). The difference between these two data sets was plotted as the specific binding curve yielding an apparent $K_d$ of 593±169 nM (mean±sem, n=4). Free CoA was able to suppress the TR-FRET signal in a concentration-dependent manner (Fig. 4F). Moreover, the TR-FRET signal was also suppressed by increasing concentrations of the CAMBD peptide, but not of a scrambled control peptide (Fig. 4F). Moreover, the CAMBD peptide also competed for recombinant mouse CaMKIIα binding to CoA-Sepharose in a concentration-dependent manner, completely preventing the interaction at concentrations >100 μM (Fig. 4G). These data show that CoA directly binds to CaMKII by a mechanism that may involve residues 290–309 in the CaMKII regulatory domain.

## Activation of CaMKII induced by CoA Requires basal $Ca^{2+}$/CAM

Since the CAMBD of CaMKII appears to interact with both CAM and CoA, we investigated the potential impact of CAM on the interaction with CoA. First, increasing concentrations of purified CaMKII or recombinant CaMKIIα were incubated with CoA-Sepharose in the absence or presence of CAM. CAM appeared to have no substantial impact on the interaction of either CaMKII preparation with CoA-Sepharose (Fig. 5A&B). The experiment in Fig. 5B was conducted in the presence of 50 μM EGTA, however this was likely not enough to completely chelate the $Ca^{2+}$ that typically contaminates all aqueous buffers. To confirm that CoA could bind directly to CaMKII independently of $Ca^{2+}$, high concentrations

of EGTA (2 mM) were used in the experiments shown in Fig. 5C, demonstrating that CoA-Sepharose can directly bind both CaMKIIα and CaMKIIγ isoforms independently of $Ca^{2+}$.

We next examined the ability of CoA, acetyl CoA and a stable CoA-thioester (CoA-propan-2-1) (Fig. S3) to directly activate CaMKIIα. While CoA stimulated CaMKII phosphorylation of caspase-2, acetyl CoA was a very weak CaMKII activator and CoApropan-2-1 did not detectably activate CaMKII (Fig. 5D). Taken together these results demonstrate that the CoA moiety is sufficient to result in CaMKII activation, and that modification of CoA, including esterification, disrupts the activation of CaMKII.

To determine whether CaMKII activation by CoA required CAM, we repeated the experiment above with or without CAM. The addition of CAM or CoA alone had no affect on CaMKII activity; however the combined addition of CoA and CAM activated CaMKII to a similar degree as saturated $Ca^{2+}$/CAM (Fig. 5E). CoA, in the presence of CAM, was also capable of activating both CaMKIIα and CaMKIIγ in the presence of low EGTA (100 μM) (Fig. 5F). Although $Ca^{2+}$ is not required for CoA binding to CaMKII, we wanted to determine whether the CoA-CAM dependent activation of CaMKII required the low levels of free $Ca^{2+}$ that are likely present in these buffers in the presence of low EGTA. Therefore, increasing concentrations of EGTA were titrated to determine whether free $Ca^{2+}$ was required for CoA-dependent activation of CaMKII. Fig. 5G shows that CaMKII activity was significantly suppressed at 500 μM and 1 mM EGTA. Therefore, CoA-induced CaMKII activation requires CAM and low concentrations of $Ca^{2+}$ (basal $Ca^{2+}$/CAM), effectively lowering the threshold for the amount of $Ca^{2+}$ required by CAM to activate CaMKII.

To determine the amount of free $Ca^{2+}$ required for CoA-dependent CaMKII activation, CaMKII activity was measured in the presence of a fixed concentration of EGTA (1 mM). We then titrated in known concentrations of "total" $CaCl_2$, resulting in CaMKII activation following addition of even 4 μM total $Ca^{2+}$ (Fig. 5H) Using the Stanford Ca-EGTA calculator (http://maxchelator.stanford.edu/CaMgATPEGTA-TS.htm), the estimated free $Ca^{2+}$ concentration with 4 μM total $Ca^{2+}$ and 1 mM EGTA under these conditions is 2.4 nM. However, the likely contamination of our buffers by about 20 μM $Ca^{2+}$ would increase free $Ca^{2+}$ concentrations to approximately 15 nM. Thus, we conclude that low nM concentrations of $Ca^{2+}$ that are typically present under basal cellular conditions partially saturate CAM (basal $Ca^{2+}$/CAM) and are required to support CoA-induced CaMKII activation, but that an increase in $Ca^{2+}$ is not required.

Activation of CaMKII by $Ca^{2+}$/CAM is cooperative, with a Hill coefficient ranging from 1.0 – 5.0 depending on the isoform and substrate used (Chao et al. 2010; Bradshaw et al. 2003). To examine whether CaMKII activation by CoA/CAM was also cooperative, we investigated the CoA concentration-dependence of CaMKIIα activation in the absence of added $Ca^{2+}$ (basal $Ca^{2+}$/CAM), based on substrate phosphorylation of GST-pro C2 (Fig. 5I) and autophosphorylation of CaMKIIα itself (Fig. 5J). The Hill coefficients (mean±sem, n=2) were 1.5±0.3 and 1.4±0.5, respectively, indicating moderate cooperativity under these conditions. Furthermore, the $K_a$ values (mean±sem, n=2) were 1.8±0.1 mM for GST-pro C2 and 0.85±0.06 mM for CaMKII phosphorylation. Together, these data demonstrate a novel, non-canonical mechanism for activation of CaMKII by CoA and CAM at low/basal levels of free $Ca^{2+}$.

## Modeling the CoA binding site on CaMKIIα

We exploited the available X-ray crystal structures of CaMKIIα(PDB:3SOA), docking algorithms with evidence that CoA interacts with the CAMBD of CaMKII, and knowledge of typical adenine ring interactions with proteins (Kuttner et al. 2003) to build a robust model of the CoA-CaMKII interaction. This model was relaxed by molecular dynamics

(MD) simulations (Fig. 6A–C). Our model predicts that the adenine ring of CoA occupies a hydrophobic pocket near L308 and makes two interactions with R300: the adenine ring stacks tightly on top of the alkyl side chain and the $NH_2$ makes a hydrogen bond to the peptide backbone carbonyl. The 3' phosphate interacts with the backbone amine of T310. The guanidine group on R296 and amino group on K300 stabilize the CoA diphosphate moiety. The pantothenate segment stacks against W214, while F293 and K292 cradle the Cys-derived segment of CoA. MD simulations reveal that addition of an acetyl group to CoA increases ligand flexibility and disrupts binding to CaMKII by destabilizing the hydrogen bond between CoA O44 and R296 (Fig. 6D, Table S1). Our data showing that the CoA moiety alone was capable of binding to and activating CaMKII (Fig. 4A&5D), and inhibiting apoptosis (Fig. 2F&G), validates this model. Taken together these data show that CoA acylation reduces binding to CaMKII.

To determine how the interaction between CoA and the CAMBD might facilitate CaMKII activation by CAM, we used MD simulations to relax the regulatory domain conformation upon CoA binding (Fig. 6C). CoA remained bound to CaMKII in five independent simulations. The CoA di-phosphate group continues to make hydrogen-bond interactions with the side chains of R296 and K300. The α-helix formed by residues 295- 300 becomes partially unwound to become a β-turn, whereas the remainder of the protein retains its structure. This occurred in all five simulations and was quantified by measuring the residue-wise secondary structural propensities during the MD production runs (Fig. S5). No such changes were observed in the absence of CoA. The conformational change resulting from this unwinding of the α-helix may be detectable by glycerol-gradient sedimentation. Incubation of CaMKIIα and CAM with CoA resulted in a modest shift in the size of CaMKII (Fig. S6B), as assessed on a 15–45% glycerol gradient. Taken together, this data supports the hypothesis that CoA binding destabilizes the secondary structure of residues 295–300. Destabilization of the regulatory domain structure may facilitate interactions with CAM under basal conditions when only 1 or 2 $Ca^{2+}$ ions are bound to CAM. Since a previous study found that CAM with only 2 $Ca^{2+}$ ions bound in the C-terminal domain can partially activate CaMKII (Shifman et al. 2006), we speculate that this then results in CaMKII activation.

The crystal structure of $Ca^{2+}$/CAM bound to CaMKIIδ(PDB ID: 2WEL) (Rellos et al. 2010) represents the activated form of CaMKII. In contrast to our model of CoA bound to the auto-inhibited form of CaMKII, K292 is solvent exposed, F293 is reoriented and buried into CAM, and R296 and K300 form salt bridges with negatively charged residues on CAM. Upon superposition of the auto-inhibited CaMKII-CoA dock pose onto the activated CaMKII-CAM bound form, the pocket for the CoA adenine ring is abolished by the protrusion of L304 (Fig. S4A&B). Moreover, to maintain interactions made by CoA ribose, diphosphate and pantothenate parts, residues R296 and K300 of CaMKII, and residues E8, E12, M145 and M146 of CAM would have to be rearranged. Therefore our model suggests that simultaneous binding of CoA and $Ca^{2+}$/CAM to CaMKII is unlikely. We validated this by showing that an excess of $Ca^{2+}$/CAM displaced CaMKII from CoA-Sepharose (Fig. 6E, Fig. S6A). We cannot rule out the possibility of a transitional CaMKII-CoA-basal $Ca^{2+}$/CAM complex. Moreover, our modeling cannot address whether CoA and CAM that is not fully saturated with $Ca^{2+}$ can bind simultaneously to the CaMKII regulatory domain since structures of basal $Ca^{2+}$/CAM or apo-CAM bound to CaMKII are not available.

Our modeling suggests that residues K292, R296, and K300 are required for CoA binding. Triple A mutants were made in the CAMBD of full-length CaMKIIα. CoA-Sepharose bound significantly less to the triple A mutant K292A/R296A/K300A CaMKIIα compared to WT CaMKIIα from cell lysates of HEK-293T cells overexpressing either the WT CaMKIIα or triple CaMKIIα mutant (Fig. 6F). Onedimensional $^{1}H$ and $^{31}P$ NMR also

showed that, compared to WT CAMBD, the triple mutant bound CoA weakly as indicated by smaller chemical shift perturbations observed during titrations (Fig. 6H). Moreover, the triple mutant CAMBD peptide did not inhibit binding of CoA-Sepharose to recombinant mouse CaMKIIα (Fig. S6C&D). Taken together, these biochemical data strongly support the prediction that amino acids K292, R296, and K300 are important for binding of CaMKII to CoA.

### NMR-guided modeling of CoA binding site on CaMKII

The interactions between the CAMBD peptide and CoA were probed by NMR spectroscopy. Assignments for CoA and the CAMBD peptides are shown in tables S3–5 and fig. 6G. NMR titrations of CoA with CAMBD indicated a weak affinity for this interaction with a $K_d$ in the 0.9 mM range (Fig. S6E). Comparison of the $^{15}N$–$^{1}H$ HSQC spectra of free and bound CAMBD indicated significant chemical shift perturbations of the backbone amides upon CoA binding observed throughout the peptide, with exception of three residues at the N-terminus and A302 (Fig. 6G). Protons of CoA that showed chemical shift perturbations were in the adenine ring, ribose sugar group and the two methyl groups of the panthothenate moiety (Fig. S6E & F, Fig. S7B and Table S5). In the $^{31}P$ spectra, the 5' diphosphate moiety showed reduced chemical shift perturbations compared to the 3' phosphate, although they both displayed similar kinetics of binding with a $K_d$ in the 0.4 mM range (Fig. 6H).

We also tested binding of CoA to full-length CaMKIIα by one-dimensional relaxation-edited $^{1}H$ NMR. In the relaxation-edited spectra, some of the CoA signals are attenuated as CoA forms a complex with the large dodecameric CaMKIIα and therefore relaxes much faster than free CoA. The relaxation-edited difference spectrum between free and CaMKII-bound CoA indicated potential additional contributions to binding also from protons of the cysteine and panthothenate moieties (Fig. S7A), attributed to CoA interactions to CaMKII outside the CAMBD region. This provides direct NMR evidence for the interaction between CoA and CaMKII.

### Coenzyme A Inhibits DHEA-Induced Apoptosis in *Xenopus* and Murine Oocytes

To determine whether CoA could activate CaMKII and suppress apoptosis in intact *X. laevis* oocytes. Our previous data showed that nutrient depletion induced by trans-dehydroandrosterone (DHEA) was sufficient to induce *X. laevis* oocyte death by a caspase-2 dependent mechanism (Nutt et al. 2005). DHEA induced oocyte apoptosis in a dose-dependent manner (Fig. 7A), and prior injection of CoA inhibited this DHEA-induced oocyte death (Fig. 7B). Moreover, the inhibitory effect of CoA was blocked by co-injection of the CAMBD peptide (Fig. 7C). Likewise, DHEA induced caspase activation in aged mouse oocytes (Fig. 7D); caspase activation and mouse oocyte death was also inhibited by prior injection of CoA (Fig. 7E, Table 1). Taken together, these findings are consistent with a model in which active metabolism maintains high levels of CoA that protect against the death of vertebrate oocytes by binding to the CaMKII regulatory domain to stimulate phosphorylation of the caspase-2. Furthermore, metabolic suppression of oocyte death by maintenance of CoA levels is conserved across vertebrates.

## DISCUSSION

We have previously identified a novel link between G6P-induced pentose phosphate pathway generation of NADPH and the cell death machinery (Nutt et al. 2005; Nutt et al. 2009; McCoy et al. 2013). We postulated that G6P/NADPH induced an active signaling system to keep these cells alive and that the default pathway, when key metabolites cannot be maintained, is cell death. In the current study, we identify the levels of CoA as a key metabolite that activates CaMKII and suppresses oocyte/egg extract apoptosis. These

findings highlight the importance of maintaining oocyte metabolism to preserve egg viability and fertility.

CoA is an essential cofactor that is found in all living organisms. Although first recognized for its role in acetylation reactions, CoA functions as an obligate cofactor in many intermediary metabolic steps. The intracellular ratio of free CoA to acyl-CoAs is tightly controlled by several mechanisms. Most CoA is concentrated in the mitochondria, where it is required for the citric acid cycle, β-oxidation, and ketogenesis (Leonardi et al. 2005). However, the 5-step CoA-synthesis pathway is localized to the cytosol, and a CoA transporter is required to shuttle CoA into mitochondria. In the first biosynthetic step, vitamin B5 (pantothenic acid) is converted to 4' phosphopanthothenic acid by pantothenate kinase (Pank), the rate-limiting enzyme in CoA synthesis. Pank has 4 human isoforms, but deletion of Pank2 leads to infertility. Mating of homozygous Pank2 females with wild-type males led to a decrease in Mendelian expectancy in the viable offspring. In contrast, mating of Pank2 males with WT females led to no viable mice because of azoospermia (Kuo 2004). These data provide strong genetic evidence for a link between CoA synthesis and preservation of fertility. Interestingly, we have ruled out the role of Pank by chemical ablation with Hopantenate (HoPAN), a robust inhibitor of Pank (Zhang et al. 2007). HoPAN treatment did not affect G6P-mediated CaMKII activation or inhibition of apoptosis. In fact our data show a novel stockpile of CoA in the form of acetyl CoA, also it is known that high activity of acyl-CoA hydrolases/thioesterases occur in vivo (Berge & Farstad 1979a; Knudsen et al. 1999). Moreover, acetyl CoA is normally found in mitochondria so our results showing that G6P-induces a significant increase of acetyl CoA in the cytosol implicates a novel metabolic circuit regulating cytosolic CoA levels, CaMKII activation, and oocyte/egg survival.

The addition of CoA recapitulated the anti-apoptotic effects of G6P at the level of CaMKII, caspase-2, and caspase-3. The concentrations of CoA added to the extract and recombinant proteins are similar to the reported cytosolic concentrations of CoA in other tissues (Robishaw & Neely 1985). Thus, our observation is physiologically relevant. However, under physiological conditions, mM concentrations of CoA are concentrated in the mitochondria, and are required for the citric acid cycle, β-oxidation, and ketogenesis (Leonardi et al. 2005). Interestingly, the mitochondria are also the signaling hub for apoptosis (Danial & Korsmeyer 2004). In *X. laevis* oocytes, caspase-2 is dormant in fresh extracts. As mitochondria are a sink for CoA we speculate that in the absence of active metabolism, mitochondria sequester CoA from the cytosol, thereby inhibiting CaMKII. This decrease in cytosolic CoA and subsequent CaMKII inhibition results in caspase-2 dephosphorylation and subsequent oocyte/egg apoptosis. Our finding that addition of G6P not only stabilizes but also increases cytosolic CoA levels provides a mechanism for G6P-mediated oocyte survival.

We propose a key part of this effect is mediated by the non-canonical CoA-dependent activation of CaMKII. There are other examples of calcium-independent CaMKII regulation, such as proteolytic cleavage of the regulatory domain (Rich et al. 1990; Kwiatkowski & King 1989). Secondly, recent studies found that CaMKII can be activated by calcium-independent binding of α-actinin (Jalan-Sakrikar et al. 2012). Finally, it has been shown that oxidation of two key methionine residues (M281 and M282) in the CaMKII regulatory domain can activate CaMKII in the absence of T286 phosphorylation (Erickson et al. 2008). Our data differs from the above in that CoA-induced CaMKII requires basal amounts of calcium. Hence, while an increase in $Ca^{2+}$ is not required, low basal concentrations of $Ca^{2+}$ are sufficient to support CoA-dependent activation of CaMKII.

Our molecular model of CoA binding to CaMKIIα is consistent with the experimental observations reported herein. The majority of the protein-ligand interactions in the model are made with the protein region spanning residues 290–309, and this peptide has been shown to be sufficient to outcompete CoA binding to full-length CaMKIIα. Acyl substitutions on CoA decrease CaMKIIα activation according to the trend CoA>acetyl-CoA>CoA-propan-2-one. In our model, the CoA sulfhydryl is oriented away from protein and towards bulk solvent where there are no accessible hydrophobic pockets. From the results of our MD simulations, we propose that modifications at this end of CoA increase ligand flexibility and disrupt binding to full-length CaMKII by destabilizing the hydrogen bond between CoA O44 and R296. These results would explain why we see the inability of acetyl CoA to bind or induce activation of CaMKII to the same extent as CoA.

Our modeling data implicate Lys292, Arg296, and Lys300 within the CAM-binding domain as key determinants of CoA binding. The NMR analysis of CoA–CAMBD peptide supported their contribution, which was further corroborated by the diminished interaction of CoA to this triple mutant CAMBD peptide. CaMKII has been extensively mutated in this region to identify regulatory determinants. A peptide-based mutagenesis study from 1992 investigated the importance of individual residues in regulating inhibitory interactions with the kinase domain (Smith et al. 1992). While mutations of Lys291, Arg297 and Lys298 displayed at least a 10-fold loss of potency, mutations of Lys292, Arg296 and Lys300 had a modest effect. Similarly, another study from 1999 investigated residues important in the auto-inhibitory interactions of the CaMKII kinase domain and regulatory domain. Mutations E285K, R296E, R298E, and K300E required significantly more $Ca^{2+}$ to achieve half-maximal kinase activity. The mutations D288K, K292E, and R297E, on the other hand, exhibited no significant changes in calmodulin binding affinity (Yang & Schulman 1999). Together, these data suggest that Lys292, Arg296 and Lys300 are largely solvent exposed, consistent with them being available for interaction with CoA, as predicted in our model and observed biochemically.

Studies using synthetic peptides and the intact CaMKII holoenzyme have yielded an excellent structural understanding of the interactions of saturated $Ca^{2+}$/CAM with the CaMKII regulatory domain. However, the potential for interactions of apo-CaM, or basal $Ca^{2+}$/CAM, with CaMKII are poorly understood. Our MD simulations show that CoA binding induces conformational changes in the C-terminal portion of the CaMKII regulatory domain, and this increased conformational flexibility may facilitate binding of perhaps basal $Ca^{2+}$/CAM. Alternatively, local conformational changes induced by CoA binding to the regulatory domain may have more far-ranging consequences to the CaMKII holoenzyme structure. Recent structural studies of CaMKII suggest that the kinase domains can adopt multiple conformations relative to the dodecameric hub of the holoenzyme. In one structure the kinase domains appear to be in a compact conformation stabilized by interactions of portions of the regulatory domain with the hub of the holoenzyme. This conformation “shields” the regulatory domain from apo-CAM and basal $Ca^{2+}$/CAM (Hudmon & Schulman 2002; Chao et al. 2011). Thus, one alternative hypothesis is that binding of CoA to the regulatory domains may destabilize the compact structure to promote a more extended kinase domain conformation that is more readily activated by basal $Ca^{2+}$/CAM. In essence, CoA acts as a wedge between the regulatory and Hub domains, destabilizing the secondary structure of the regulatory domain enough to expose C-terminal residues such that basal $Ca^{2+}$/CAM can bind and displace CoA. Furthermore, our model predicted CoA binding decreased alpha helical propensity at residues 295–300 and our biochemical data demonstrating the ability of CoA to alter the sedimentation properties of CaMKII in a glycerol gradient support this model.

The study of metabolic regulation in mammalian cells is cumbersome, as it is not feasible to introduce intermediate metabolites directly into cells unless by microinjection. Therefore, using the Xenopus oocyte model allowed us to discover a novel connection between metabolism and oocyte viability. A better understanding of the molecular mechanisms underlying these links might provide the basis for developing novel strategies for CoA in promoting oocytes longevity for increased fertility.

## EXPERIMENTAL PROCEDURES

### Preparation of Xenopus Oocytes, Extracts, Cytosols

Mature female frogs were induced to lay eggs as previously described (Smythe & Newport 1991). Egg extracts were prepared as described previously (Nutt et al. 2009).

Stage VI oocytes were harvested from mature female frogs as described previously (Nutt et al. 2009). Healthy stage VI oocytes were selected for microinjection and treatment.

### Recombinant Protein Cloning and Expression

N-terminally GST-tagged (pGEX-KG) *Xenopus* wild type caspase-2 pro-domain was expressed in, and purified from, BL21 *E. coli* as previously described (E. K. Evans et al. 1997). *Xenopus* caspase-2 constructs were cloned into pGEX-KG and pSP64T as previously described (Nutt et al. 2005). Recombinant mouse CaMKIIα was prepared as described previously (Brickey et al. 1990). Mouse CaMKIIα WT and K292A/R296A/K300A mutant constructs (pcDNA3) for transfecting into HEK-293T cells were generated using primers described in Extended Experimental Procedures.

### Caspase 3/7 Assay

Caspase-3/7 activity in extracts was analyzed similar to as previously described (Nutt et al 2005). For this study, a luminescent substrate (Caspase-Glo 3/7 Assay, Promega) was used.

### Kinase Assays

GST-tagged *Xenopus* caspase-2 pro-domain (GST-pro C2) bound to glutathione- Sepharose was incubated in egg extract, cytosol or heat soluble cytosol with 5 μCi [$\gamma$-$^{32}$P]ATP, ± indicated treatments for 2 hours (unless otherwise stated) at room temp. GSTPro C2 beads were analyzed by autoradiography.

*In vitro* kinase assays were performed by incubating glutathione-Sepharose bound GSTpro C2 in kinase buffer with, CaMKII ± calmodulin, in the presence of 5μCi [$\gamma$-$^{32}$P]ATP. Reactions were incubated ± EGTA and ± indicated treatments at room temp. for 30 min.

### Coupled-Sepharose Binding Assays

CoA, acetyl CoA, NADPH or CAM conjugated to Sepharose were incubated in egg extract for 45 min. at room temp. Beads were washed and analyzed by immunoblotting.

*In vitro* binding experiments were performed by incubating CoA-Sepharose, or CAM-Sepharose in kinase buffer with unless otherwise stated, mouse CaMKIIα ± calmodulin, for 30 min. at room temp, ± EGTA. For CAM-Sepharose binding, kinase buffer was supplemented with $CaCl_2$. Beads were washed and analyzed by SDS-PAGE and immunoblotting.

### Xenopus Oocyte Microinjections

Stage VI oocytes were microinjected with either vehicle control 5 mM CoA, 20 mM CoA, or 20 mM CoA and 1mM CAMBD. Injected oocytes were subsequently incubated with vehicle control or indicated concentrations of DHEA in OR-2 buffer (Nutt et al 2009), at 18°C and monitored for induction of apoptosis.

### Extended Experimental Procedures

Additional and more detailed experimental procedures, including a list of antibodies and reagents used, can be found in the Supplemental Information.

## Supplementary Material

Refer to Web version on PubMed Central for supplementary material.

## Acknowledgments

The authors would like to thank Dr. Sara Gragg for her support and guidance and Changli He for technical support. This work was supported by the V Foundation, the American Lebanese Syrian Associated Charities (ALSAC), and National Cancer Institute of the National Institutes of Health under Award Number P30CA021765. RJC was supported by NIH award R01MH063232. The content is solely the responsibility of the authors and does not necessarily represent the official views of the National Institutes of Health.

## REFERENCES

Backs J, et al. The γ isoform of CaM kinase II controls mouse egg activation by regulating cell cycle resumption. Proceedings of the National Academy of Sciences. 2010; 107(1):81–86.

Berge RK, Farstad M. Dual localization of long-chain acyl-CoA hydrolase in rat liver: one in the microsomes and one in the mitochondrial matrix. European journal of biochemistry / FEBS. 1979a; 95(1):89–97. [PubMed: 37074]

Berge RK, Farstad M. Purification and characterization of long-chain acyl-CoA hydrolase from rat liver mitochondria. European journal of biochemistry / FEBS. 1979b; 96(2):393–401. [PubMed: 37085]

Bergeron L, et al. Defects in regulation of apoptosis in caspase-2-deficient mice. Genes & development. 1998; 12(9):1304–1314. [PubMed: 9573047]

Bradshaw JM, et al. An ultrasensitive $Ca^{2+}$/calmodulin-dependent protein kinase II-protein phosphatase 1 switch facilitates specificity in postsynaptic calcium signaling. Proceedings of the National Academy of Sciences of the United States of America. 2003; 100(18):10512–10517. [PubMed: 12928489]

Brickey DA, et al. Expression and characterization of the alpha-subunit of $Ca^{2+}$/calmodulin-dependent protein kinase II using the baculovirus expression system. Biochemical and biophysical research communications. 1990; 173(2):578–584. [PubMed: 2175600]

Chao LH, et al. A Mechanism for Tunable Autoinhibition in the Structure of a Human $Ca^{2+}$/Calmodulin-Dependent Kinase II Holoenzyme. Cell. 2011; 146(5):732–745. [PubMed: 21884935]

Chao LH, et al. Intersubunit capture of regulatory segments is a component of cooperative CaMKII activation. Nature Publishing Group. 2010; 17(3):264–272.

Danial NN, Korsmeyer SJ. Cell death: critical control points. Cell. 2004; 116(2):205–219. [PubMed: 14744432]

Deberardinis RJ, et al. Beyond aerobic glycolysis: transformed cells can engage in glutamine metabolism that exceeds the requirement for protein and nucleotide synthesis. Proceedings of the National Academy of Sciences of the United States of America. 2007; 104(49):19345–19350. [PubMed: 18032601]

Dworkin MB, Dworkin-Rastl E. Metabolic regulation during early frog development: glycogenic flux in Xenopus oocytes, eggs, and embryos. Developmental Biology. 1989; 132(2):512–523. [PubMed: 2538374]

Erickson JR, et al. A Dynamic Pathway for Calcium-Independent Activation of CaMKII by Methionine Oxidation. Cell. 2008; 133(3):462–474. [PubMed: 18455987]

Evans EK, et al. Crk is required for apoptosis in Xenopus egg extracts. EMBO. 1997; 16(2):230–241.

Gosden RG. Prospects for Oocyte Banking and In Vitro Maturation. Journal of the National Cancer Institute Monographs. 2005; 2005(34):60–63. [PubMed: 15784826]

Hudmon AA, Schulman HH. Structure-function of the multifunctional Ca2+/calmodulin-dependent protein kinase II. The Biochemical journal. 2002; 364(Pt 3):593–611. [PubMed: 11931644]

Jalan-Sakrikar N, et al. Substrate-selective and Calcium-independent Activation of CaMKII by α-Actinin. Journal of Biological Chemistry. 2012; 287(19):15275–15283. [PubMed: 22427672]

Johnson J, et al. Germline stem cells and follicularrenewal in the postnatal mammalianovary. 2004:1–7.

Knudsen J, et al. Role of acylCoA binding protein in acylCoA transport, metabolism and cell signaling. Molecular and cellular biochemistry. 1999; 192(1–2):95–103. [PubMed: 10331663]

Kuo YM. Deficiency of pantothenate kinase 2 (Pank2) in mice leads to retinal degeneration and azoospermia. Human Molecular Genetics. 2004; 14(1):49–57. [PubMed: 15525657]

Kuttner YY, et al. A consensus-binding structure for adenine at the atomic level permits searching for the ligand site in a wide spectrum of adenine-containing complexes. Proteins: Structure, Function, and Bioinformatics. 2003; 52(3):400–411.

Kwiatkowski APA, King MMM. Autophosphorylation of the type II calmodulin-dependent protein kinase is essential for formation of a proteolytic fragment with catalytic activity. Implications for long-term synaptic potentiation. Biochemistry (Washington). 1989; 28(13):5380–5385.

Leonardi R, et al. Coenzyme A: Back in action. Progress in Lipid Research. 2005; 44(2–3):125–153. [PubMed: 15893380]

Lobo RA. Potential options for preservation of fertility in women. The New England journal of medicine. 2005; 353(1):64–73. [PubMed: 16000356]

McCoy F, et al. Metabolic Regulation of CaMKII Protein and Caspases in Xenopus laevis Egg Extracts. Journal of Biological Chemistry. 2013; 288(13):8838–8848. [PubMed: 23400775]

Nutt LK. The Xenopus oocyte: a model for studying the metabolic regulation of cancer cell death. Seminars in cell & developmental biology. 2012; 23(4):412–418. [PubMed: 22507445]

Nutt LK, et al. Metabolic Control of Oocyte Apoptosis Mediated by 14-3-3ζ-Regulated Dephosphorylation of Caspase-2. Developmental Cell. 2009; 16(6):856–866. [PubMed: 19531356]

Nutt LK, et al. Metabolic Regulation of Oocyte Cell Death through the CaMKIIMediated Phosphorylation of Caspase-2. Cell. 2005; 123(1):89–103. [PubMed: 16213215]

Perez GIG, et al. Apoptosis-associated signaling pathways are required for chemotherapy-mediated female germ cell destruction. Nature Medicine. 1997; 3(11):1228–1232.

Reitzer LJ, Wice BM, Kennell D. Evidence that glutamine, not sugar, is the major energy source for cultured HeLa cells. The Journal of biological chemistry. 1979; 254(8):2669–2676. [PubMed: 429309]

Rellos P, et al. Structure of the CaMKIIδ/Calmodulin Complex Reveals the Molecular Mechanism of CaMKII Kinase Activation S.S. Taylor, ed. PLoS Biology. 2010; 8(7):e1000426. [PubMed: 20668654]

Rich DPD, et al. Proteolytic activation of calcium/calmodulin-dependent protein kinase II: Putative function in synaptic plasticity. Molecular and Cellular Neuroscience. 1990; 1(2):107–116. [PubMed: 19912759]

Robishaw JD, Neely JR. Coenzyme A metabolism. The American journal of physiology. 1985; 248(1 Pt 1):E1–E9. [PubMed: 2981478]

Shifman JM, et al. $Ca^{2+}$/calmodulin-dependent protein kinase II (CaMKII) is activated by calmodulin with two bound calciums. Proceedings of the National Academy of Sciences of the United States of America. 2006; 103(38):13968–13973. [PubMed: 16966599]

Smith MKM, et al. Functional determinants in the autoinhibitory domain of calcium/calmodulin-dependent protein kinase II. Role of His282 and multiple basic residues. The Journal of biological chemistry. 1992; 267(3):1761–1768. [PubMed: 1309796]

Smythe C, Newport JW. Systems for the study of nuclear assembly, DNA replication, and nuclear breakdown in Xenopus laevis egg extracts. Methods in cell biology. 1991; 35:449–468. [PubMed: 1664032]

Warburg O. On the origin of cancer cells. Science. 1956; 123(3191):309–314.0. [PubMed: 13298683]

Wellen KE, et al. ATP-Citrate Lyase Links Cellular Metabolism to Histone Acetylation. Science. 2009; 324(5930):1076–1080. [PubMed: 19461003]

Yang E, Schulman H. Structural examination of autoregulation of multifunctional calcium/calmodulin-dependent protein kinase II. The Journal of biological chemistry. 1999; 274(37):26199–26208. [PubMed: 10473573]

Zhang Y-M, et al. Chemical knockout of pantothenate kinase reveals the metabolic and genetic program responsible for hepatic coenzyme A homeostasis. Chemistry & Biology. 2007; 14(3): 291–302. [PubMed: 17379144]

## Highlights

- CoA directly binds to the regulatory domain of CaMKII.
- CoA activates CaMKII in a calmodulin-dependent manner.
- CoA inhibits apoptosis in both *X. laevis* and *Murine* oocytes.

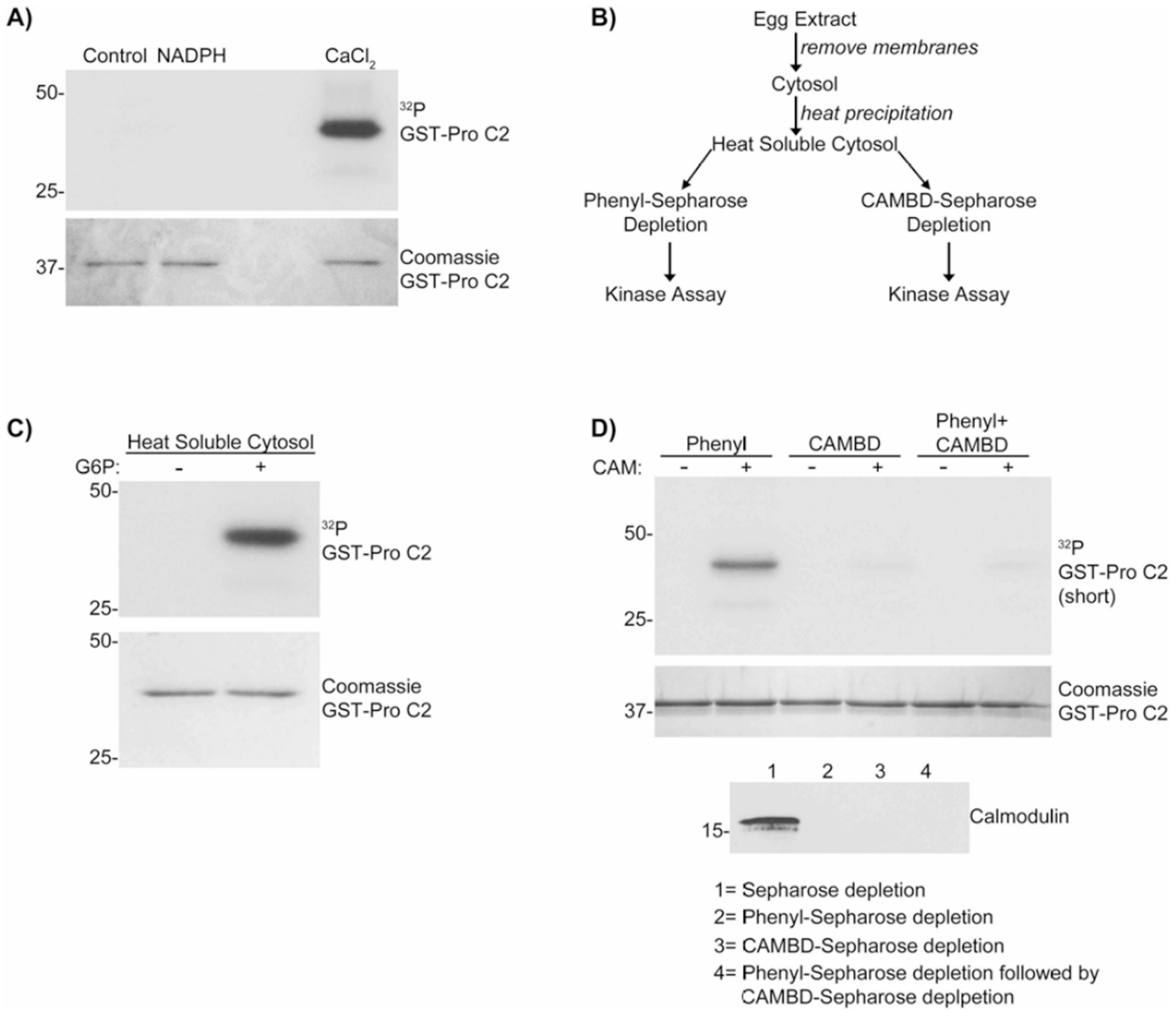


**Figure 1. G6P activates a heat soluble cytosolic factor responsible for CaMKII activation**

A) Glutathione-Sepharose bound caspase-2 pro-domain (GST-pro C2) was incubated in kinase buffer with [γ-$^{32}$P]ATP, CaMKIIα, CAM, ± 5 mM NADPH or 50 μM $CaCl_2$. Beads were analyzed by autoradiography. n= 2.

B) *Scheme used to characterize the factor responsible for CaMKII activation.*

C) GST-pro C2 was incubated in heat soluble cytosol prepared ± G6P, supplemented with CaMKIIα in the presence of [γ-$^{32}$P]ATP. Beads were analyzed as in panel A. n≥3.

D) (Top panel) GST-pro C2 was incubated in heat soluble cytosols depleted with either Phenyl-Sepharose, CAMBD-Sepharose, or serially depleted with Phenyl-Sepharose followed by CAMBD-Sepharose, with CaMKIIα, [γ-$^{32}$P]ATP, ± CAM for 30 min. Beads were analyzed as in panel A. (Lower panel) Depletion of CAM was confirmed by immunoblotting. n≥3.

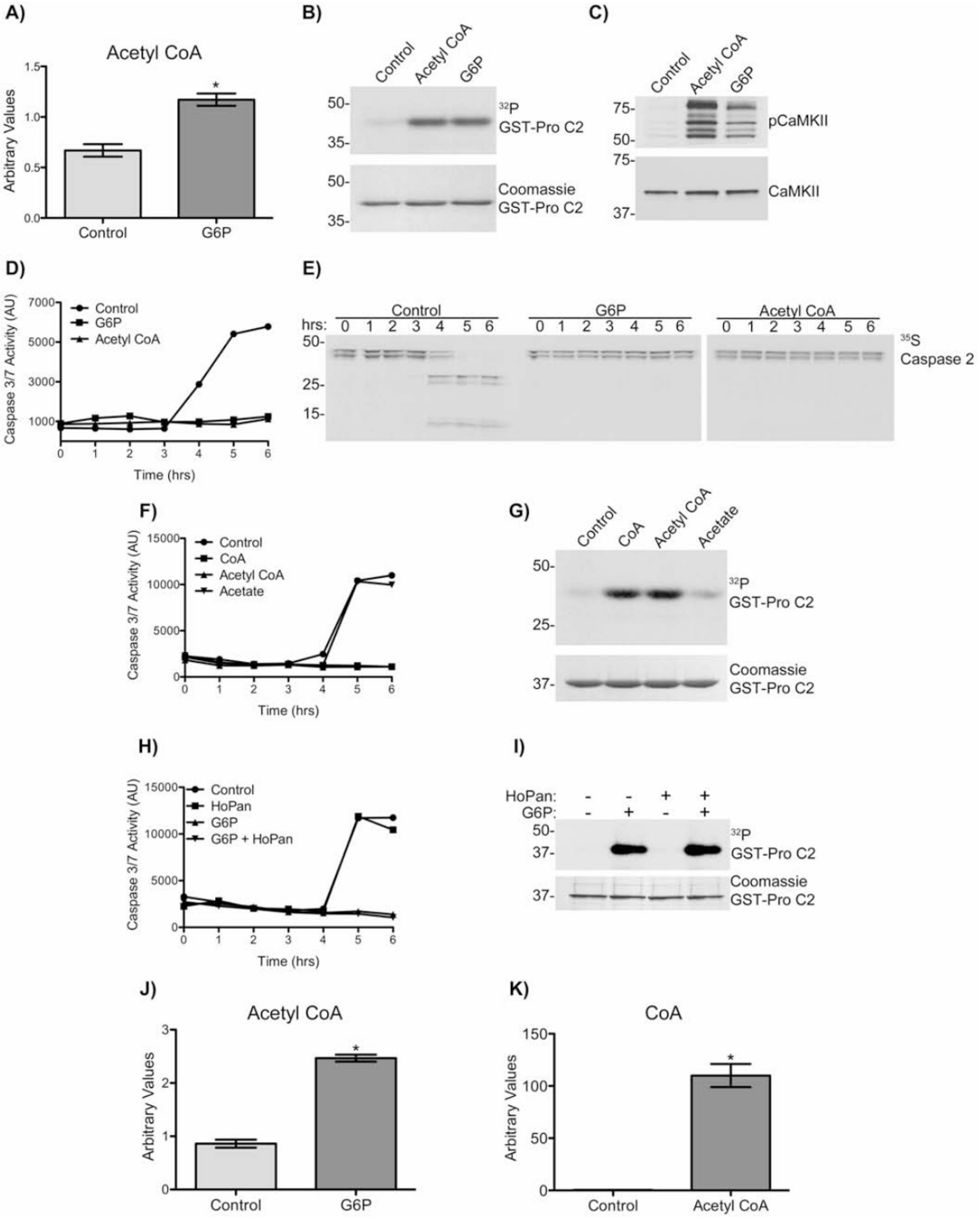


**Figure 2. G6P increases cytosolic levels of acetyl CoA**

A) Cytosolic acetyl CoA levels of extracts treated ± G6P were measured at 0 hr. Each bar represents mean ± S.E. of n= 5. * indicates a p-value <0.05. Also see Figs. S1&2.

B) GST-pro C2 was incubated in extract with 10 mM acetyl CoA or 20 mM G6P, and [$\gamma$-$^{32}$P]ATP. Beads were analyzed by autoradiography. n≥3.

C) Extracts were incubated with 10 mM acetyl CoA, or 20 mM G6P, for 2 hrs. Samples were immunoblotted for pCaMKII T286/287 and total CaMKII. n≥3.

D) Extracts were incubated with 10mM acetyl CoA or 20 mM G6P. Samples were taken at indicated times and analyzed for caspase-3/7 activity. n≥3.

E) Extracts supplemented with $^{35}$S-labeled caspase-2, was incubated ± 10 mM acetyl CoA or 20 mM G6P. Samples were taken at indicated times and analyzed by autoradiography. Note appearance of cleaved caspase-2 products at 4–6 hours in control samples, and their absence in G6P and acetyl CoA samples. n=2.
F) Extracts were incubated with CoA, acetyl CoA, acetate (all 10 mM) or 20 mM G6P. Samples were taken at indicated times and analyzed for caspase-3/7 activity. n=2.
G) GST-pro C2 was incubated in extract with CoA, acetyl CoA or acetate (all 10 mM), and [$\gamma$-$^{32}$P]ATP. Beads were analyzed by autoradiography. n=2.
H) Extracts were incubated with 20 mM G6P alone, 200 μM HoPan alone, or G6P+HoPan. Samples were taken at indicated times and analyzed for caspase-3/7 activity. n=2.
I) Glutathione-Sepharose bound GST-pro C2 was incubated in extract with 20 mM G6P alone, 200 μM HoPan alone, or G6P+HoPan, and [$\gamma$-$^{32}$P]ATP. Beads were analyzed by autoradiography. n=2.
J) Heat soluble fractions of cytosols treated ± 20 mM G6P were prepared and acetyl CoA levels analyzed by LC/MS/MC, using a method independent form that used in panel A. Each bar represents mean ± S.E. of n= 3* indicates a p-value <0.05.
K) Heat soluble fractions of cytosols treated with or without 10 mM acetyl CoA were prepared and CoA levels analyzed by LC/MS/MS, using a method independent form that used in fig. 3A. Each bar represents mean ± S.E. of n= 3 * indicates a p-value <0.05.

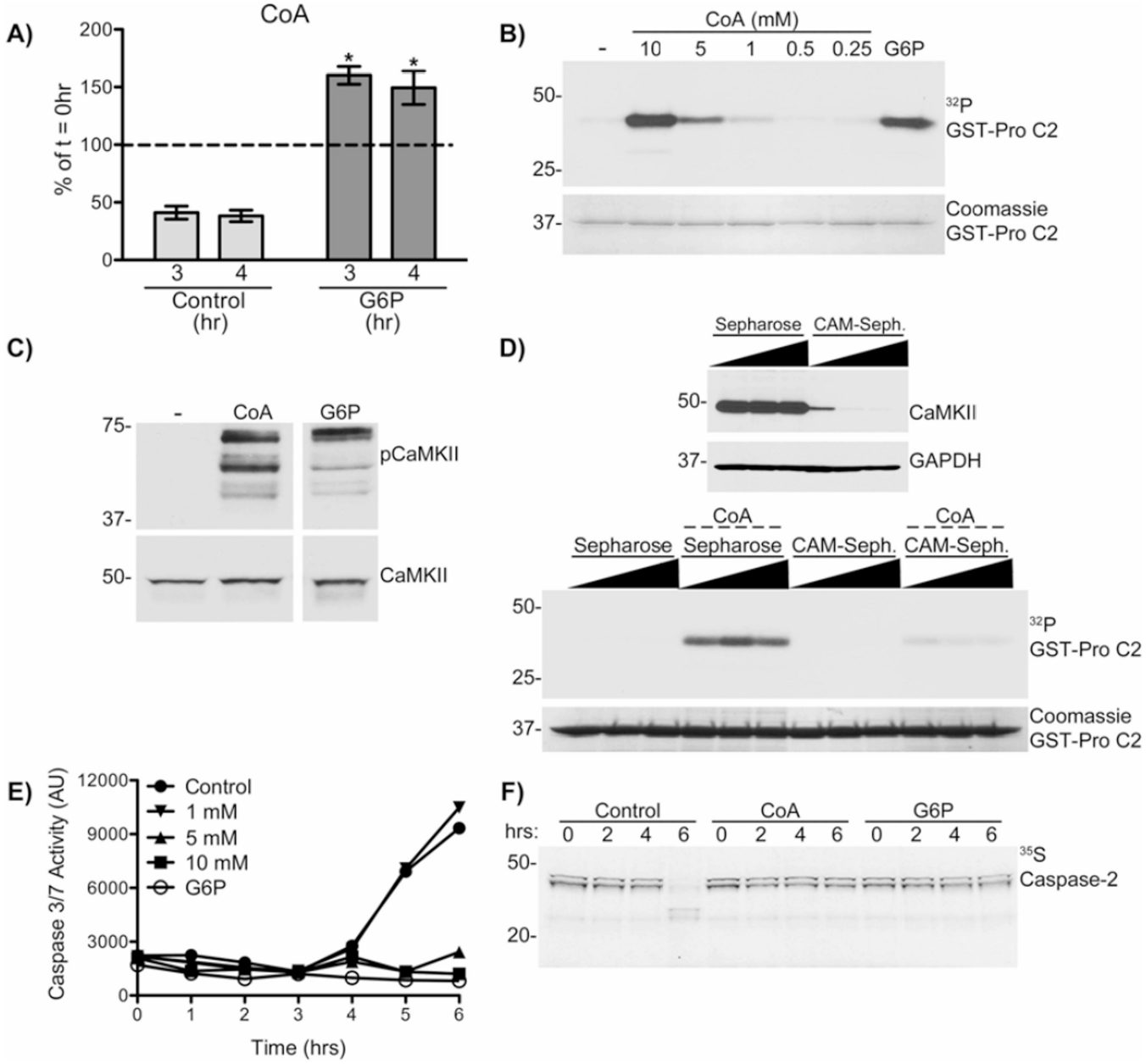


**Figure 3. Increased cytosolic CoA following G6P activates CaMKII and inhibits apoptosis**

A) Cytosolic CoA levels of extracts treated ± G6P were measured at indicated time points. Each bar represents mean ± S.E. of n= 5, expressed as % of 0 hr (Control 0 hr and G6P 0 hr respectively). * indicates a p-value <0.05 for G6P 3 and 4 hr relative to control.

B) GST-pro C2 was incubated in extract with indicated concentrations of CoA or 20 mM G6P, and [$\gamma$-$^{32}$P]ATP. Beads were analyzed by autoradiography. n≥3.

C) Extracts were incubated with 10 mM CoA, or 20 mM G6P, for 2 hrs. Samples were immunoblotted for pCaMKII T286/287 and total CaMKII. n≥3.

D) (Top panel) 3 separate aliquots of extract were depleted using 3 separate bead amounts of Sepharose or CAM-Sepharose. (Lower panel) GST-pro C2 was incubated in the depleted extracts with [$\gamma$-$^{32}$P]ATP ± 10 mM CoA. Beads were analyzed as in panel B. n= 2.

E) Extracts were incubated with indicated concentrations of CoA or 20 mM G6P. Samples were taken at indicated times and analyzed for caspase-3/7 activity. n≥3.
F) Extracts supplemented with $^{35}$S-labeled caspase-2, were incubated ± 10mM CoA or 20mM G6P. Samples were taken at indicated times and analyzed by autoradiography. Note the appearance of cleaved caspase-2 products at 6 hours in control samples, and their absence in G6P and CoA samples. n=2.

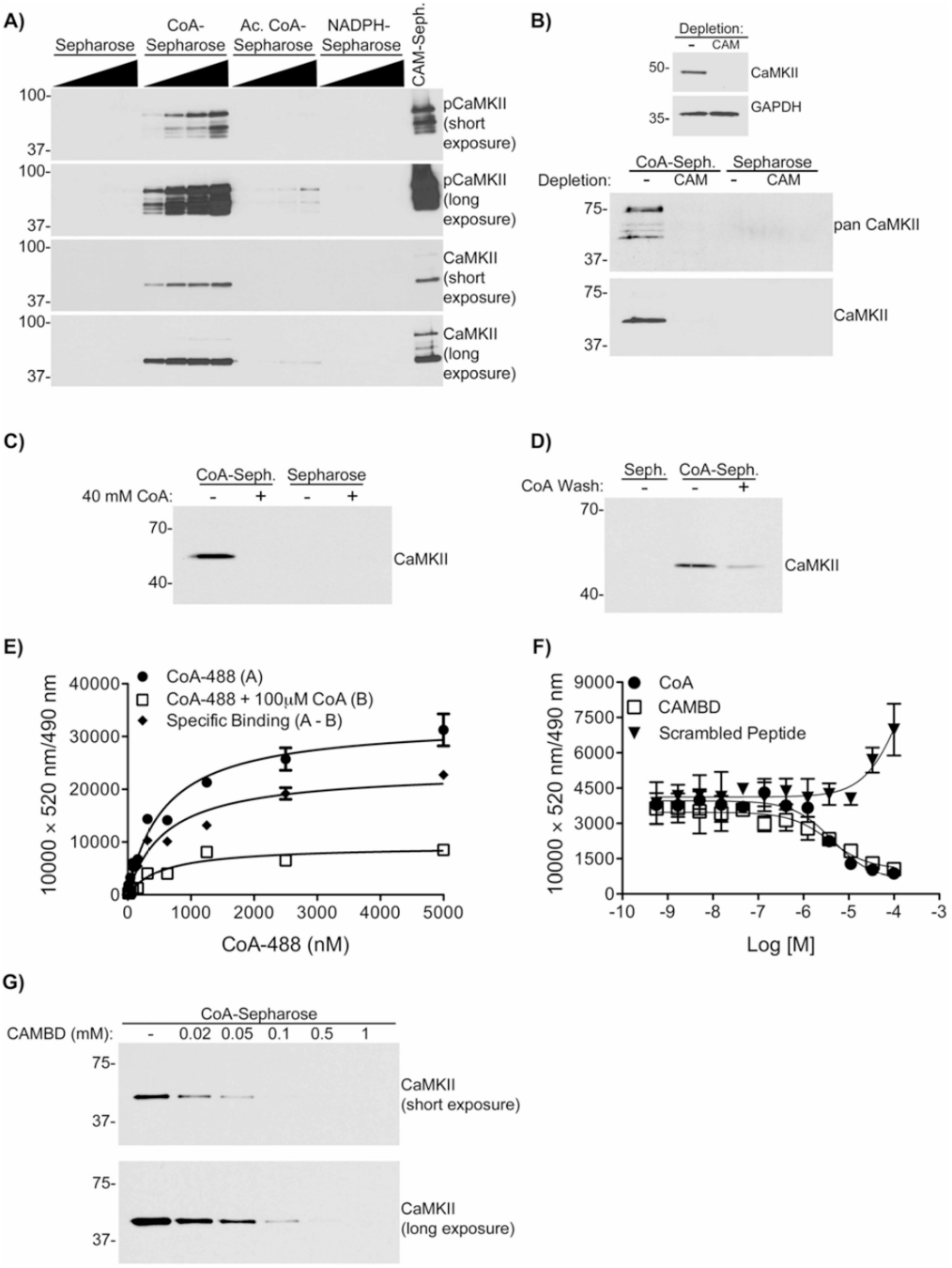


**Figure 4. CoA binds endogenous CaMKII in *X. laevis* egg extracts, and directly *in vitro***

A) CoA-Sepharose, acetyl CoA-Sepharose (Ac. CoA-Sepharose), NADPH-Sepharose, CAM-Sepharose or Sepharose alone were incubated in extracts. Beads were immunoblotted for CaMKII and pCaMKII T286/287. Two separate exposures are shown. n=3.

B) (Top panel) Extracts were depleted with Sepharose or CAM-Sepharose as in Fig. 2F. (Lower panel) Depleted extracts were incubated with CoA-Sepharose or Sepharose alone and analyzed as in panel A, but also immunoblotting with a panCaMKII antibody. n=2.

C) *CoA saturated egg extract blocks CaMKII binding to CoA.* CoA-Sepharose or Sepharose alone were incubated in extracts supplemented ± 40 mM CoA and analyzed as in panel A. n=3

D) CoA-Sepharose or Sepharose alone were incubated in extracts, washed ± 25 mM CoA, and analyzed as in panel A. n=2.

E) CoA-488 was incubated with His-CaMKIIα and Tb-anti-His, ± 100 μM CoA, and analyzed by TR-FRET. A (filled circles) = an increase in FRET signal by CoA alone. B (open squares) = excess CoA present. The difference between these two data sets was plotted as the specific binding curve (A–B, filled diamonds) Each data point represents a mean±S.D. of n=4.

F) CoA-488 was incubated with human His-CaMKIIα and Tb-anti-His, in the presence of indicated concentrations of CoA, CAMBD, or calmodulin inhibitory control peptide and analyzed by TR-FRET. Each data point represents a mean±S.D. of n=4.

G) CoA-Sepharose was incubated in kinase buffer with 30 nM CaMKIIα, and indicated concentrations of CAMBD, in the presence of 50 μM EGTA. Beads were immunoblotted for CaMKIIα. n=3.

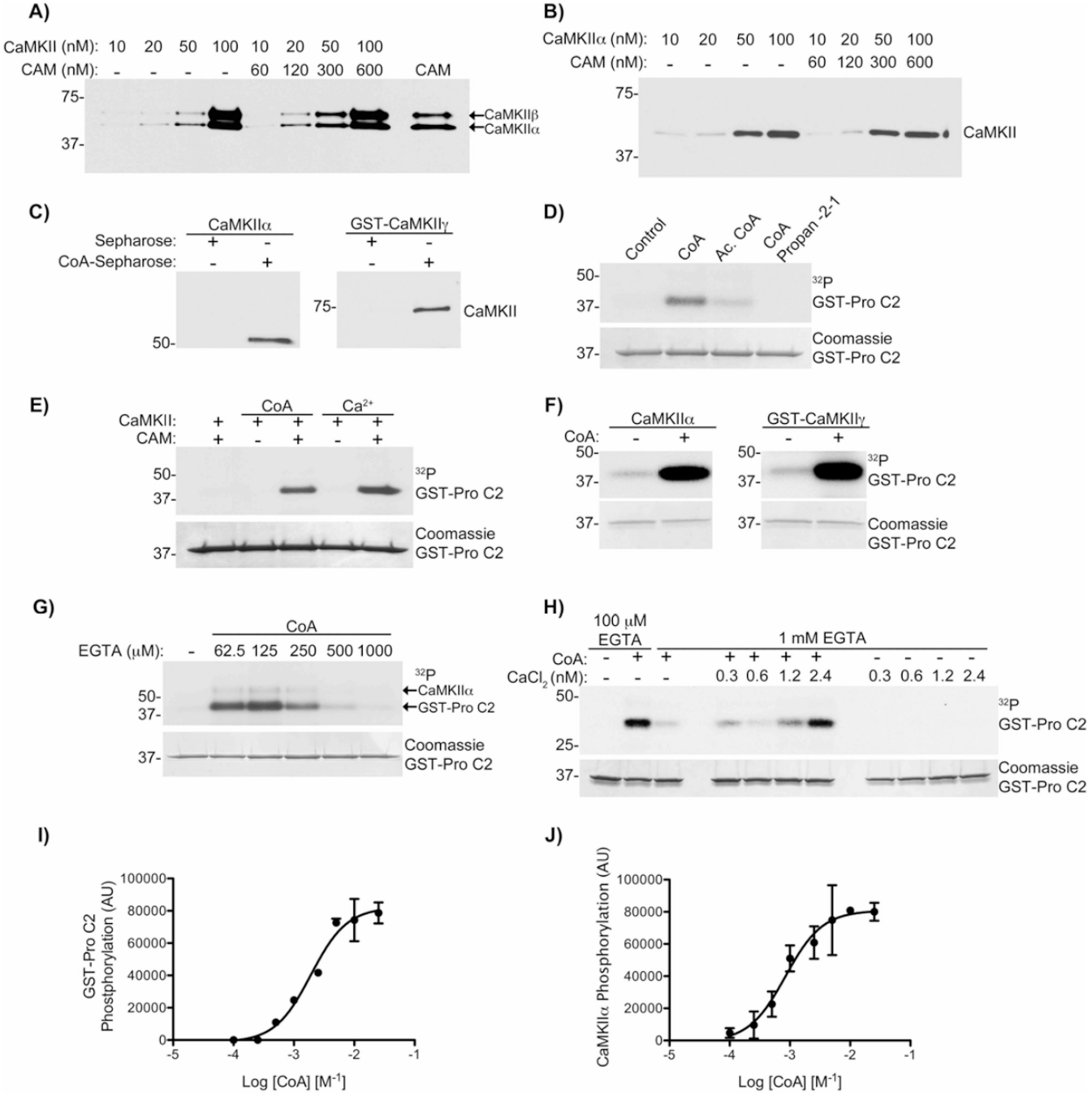


**Figure 5. CaMKII activation induced by CoA requires basal $Ca^{2+}$/CAM**

A) CoA-Sepharose was incubated with indicated concentrations of rat brain purified CaMKII ± CAM in kinase buffer. CAM-Sepharose was incubated with 100 nM of CaMKII as a positive control (last lane). Beads were immunoblotted for CaMKII. n≥3.

B) The experiment from panel A was repeated using recombinant mouse CaMKIIα, and in the presence of 50 μM EGTA. n≥3.

C) CoA-Sepharose was incubated with 65.6 nM of mouse CaMKIIα (left panel), or 65.6 nM human GST-CaMKIIγ (right panel) in kinase buffer in the presence of 2 mM EGTA. Beads were analyzed as in panel A. n=2.

D) GST-pro C2 was incubated in kinase buffer with [γ-$^{32}$P]ATP, mouse CaMKIIα, CAM and either CoA, acetyl CoA (Ac. CoA) or CoA-propan-2-1 (all 10 mM), in the presence of 50 μM EGTA. Beads were analyzed by autoradiography. n=2 (also see Fig. S3).
E) GST-pro C2 was incubated in kinase buffer with [γ -$^{32}$P]ATP and rat brain purified CaMKII, ± CAM, 10 mM CoA or 500 μM $CaCl_2$. Beads analyzed as in panel D. n≥3.
F) GST-pro C2 was incubated in kinase buffer with [γ-$^{32}$P]ATP, mouse CaMKIIα (left), human GST-CaMKIIγ (right), CAM and 10 mM CoA, in the presence of 100 μM EGTA. Beads were analyzed as in panel D. n=2.
G) GST-pro C2 was incubated in kinase buffer with [γ-$^{32}$P]ATP, mouse CaMKIIα, CAM, 10 mM CoA and indicated concentrations of EGTA. Beads were analyzed as in panel D. n=3.
H) GST-pro C2 was incubated in kinase buffer with [γ-$^{32}$P]ATP, CaMKIIα, CAM, CoA, ± indicated concentrations of $CaCl_2$, and either 100 μM EGTA or 1 mM EGTA. Beads were analyzed as in panel D. n=3.
I) GST-pro C2 was incubated with [γ-$^{32}$P]ATP, CaMKIIα, CAM and indicated concentrations of CoA, in the presence of 50 μM EGTA. Beads were analyzed as in panel D. Each data point represents mean ± S.E. of 2.
J) The same experiment as in panel H, assessing the phosphorylation of CaMKIIα. Each data point represents mean ± S.E. of 2.

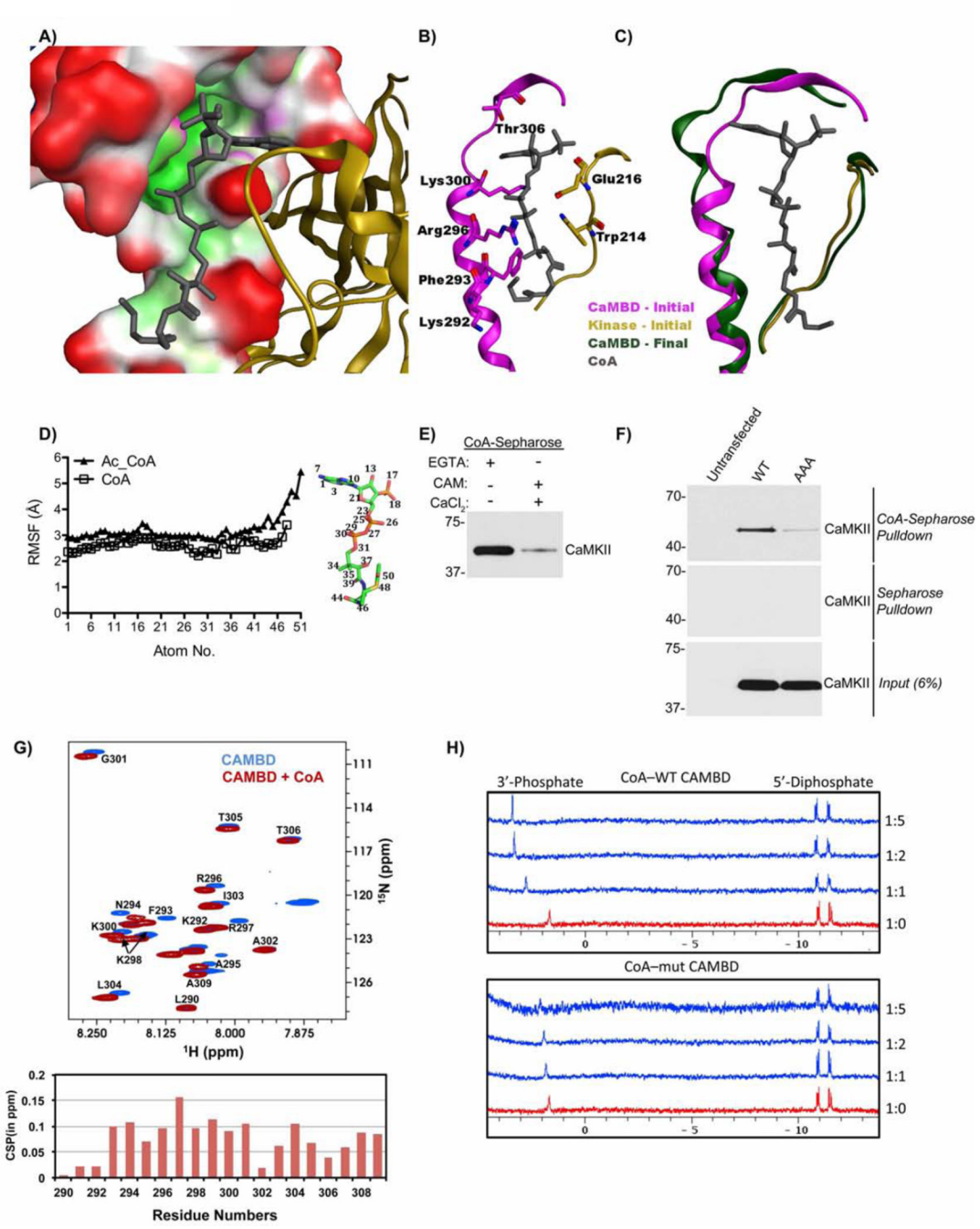


**Figure 6. CoA interacts with the CAMBD of CaMKII and requires residues K292/R296/K300**

A) Pocket surface representation of the docked model of CaMKII-CoA. B) Wire representation of pose in panel A highlighting protein residues that make direction interactions with CoA. View has been rotated for clarity. C) CaMKIIα-CoA complex (green) following MD simulation showing unwinding at the residues 295–300 of the regulatory domain. The kinase domain is colored yellow, CAMBD as magenta, the Hub domain is blue and CoA in grey. A portion of the CaMKIIα structure is hidden for clarity (also see Fig. S4&5)

D) Atom-wise Root Mean Square Fluctuations (RMSF) of CoA (Red) and acetyl-CoA (Blue) averaged over five MD independent simulations. Each data point represents the mean of 5 independent simulations.
E) CoA-Sepharose beads were incubated in kinase buffer with 100 nM CaMKIIα, in the presence of 100 μM EGTA and absence of $CaCl_2$/CAM, or in the presence of 1 mM $CaCl_2$ and 1 μM calmodulin and absence of EGTA. Beads were immunoblotted for CaMKII. n=2.
F) Lysates of HEK-293T cells transfected with wild type (WT) mouse CaMKIIα, or mouse CaMKIIα K292A/R296A/K300A (AAA) were incubated with CoA-Sepharose, or Sepharose, in the presence of 2 mM EGTA. Beads were analyzed as in panel E. Input samples were also blotted for CaMKII to confirm equal transfection efficiencies. n≥3.
G) (Top panel) $^{15}N$–$^{1}H$ HSQC spectra of 2 mM WT CAMBD peptide ± 10-fold excess CoA measured using the natural abundance of the $^{15}N$ isotope. (Lower panel) $^{15}N$–$^{1}H$ chemical shift perturbations (CSPs) versus CAMBD residue numbers for the samples above.
H) $^{31}P$ NMR titrations of 200 μM CoA with 1, 2, 5 molar equivalents of WT and K292A/R296A/K300A mutant CAMBD peptide. (see Supp. Figs. 6&7).

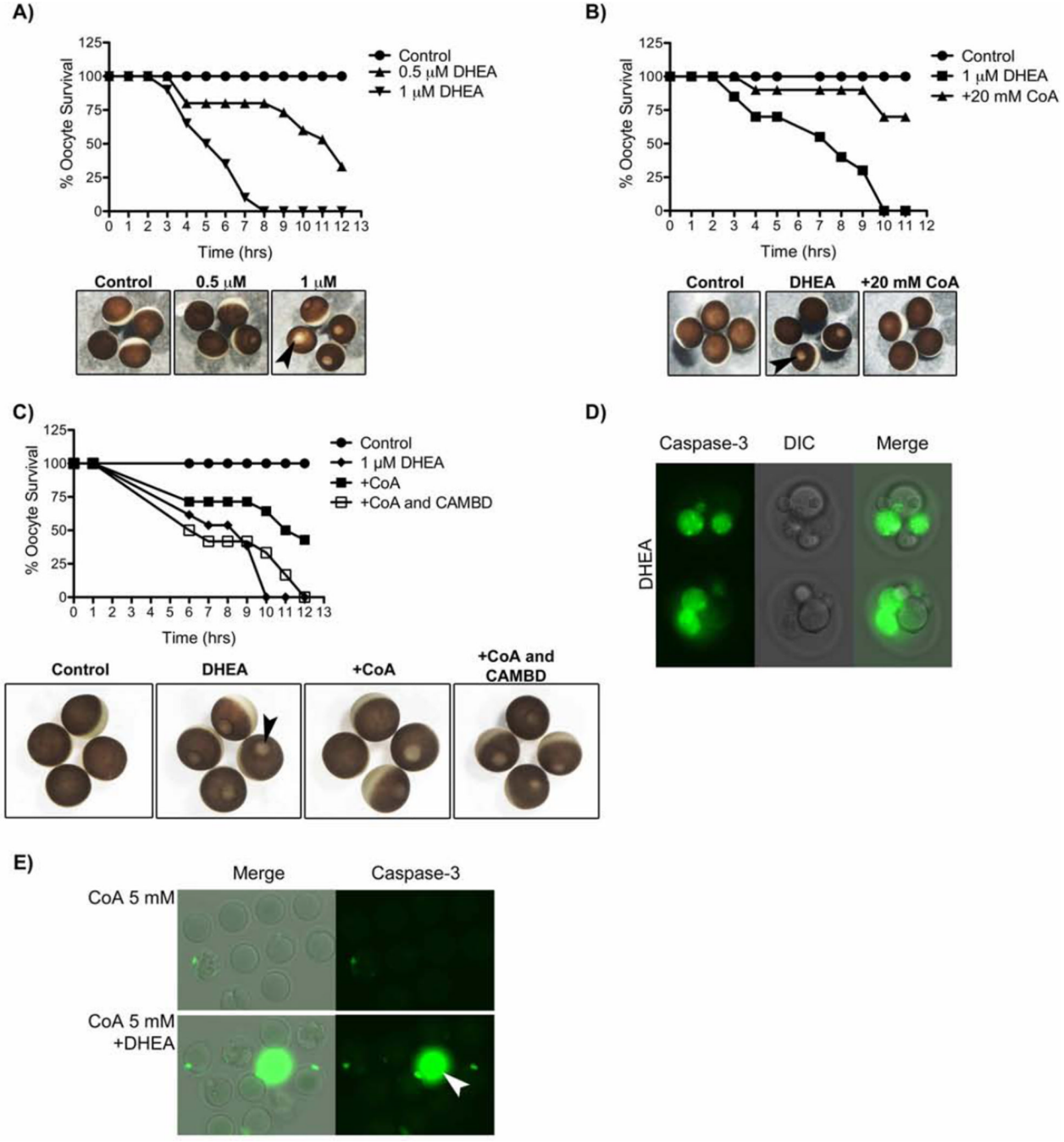


**Figure 7. CoA inhibits DHEA induced death in *Xenopus* and mouse oocytes**

A) Stage VI oocytes were incubated in vehicle control, or indicated concentrations of DHEA, and monitored for induction of apoptosis at indicated times. Below, are representative images of oocytes at 8 hrs. Black arrowhead illustrates an example oocyte undergoing apoptosis, indicated by the appearance of the 'white dot' on the animal pole.

B) Stage VI oocytes were injected with either vehicle control or 20 mM CoA and incubated in the presence or absence of 1 μM DHEA. Oocytes were monitored for induction of apoptosis at indicated times. Below, are representative images of oocytes at 7 hrs.

C). Stage VI oocytes were injected with either vehicle control, 20 mM CoA alone, or 20 mM CoA and 1 mM CAMBD peptide, and incubated in the presence or absence of 1 μM DHEA.

Oocytes were monitored for induction of apoptosis at indicated times. Below, are representative images of oocytes at 11 hrs.

D) Mouse oocytes were aged for 12 hrs, incubated in 100 μM DHEA for 12 hours, and stained for caspase-3 activity. See Table 1 for more details.

E) Mouse oocytes were microinjected with 5 mM CoA, aged for 12 hrs and then incubated ± 100 μM DHEA. Oocytes were stained for caspase-3 activity. The white arrowhead indicates an area of non-specific staining. See table 1 for more details.

## Table 1

### CoA inhibits DHEA induced death in aged mouse oocytes

Mouse oocytes were injected with vehicle control or indicated concentrations of CoA. Injected oocytes were subsequently aged by incubation in KSOM supplemented with 0.1% PVA for 12 hrs, prior to incubation in the absence or presence of 100 μM DHEA for a further 12 hrs, and monitored for morphological changes. The significance of the difference between the treatment groups was tested using the Chi-square test. A p-value of $<0.05$ was considered significant. A significant difference between the treatment groups ($p<0.0001$) was observed. Oocytes were also stained with caspase-3 antibody. (See Figure 7).

| Treatment | | |
|---|---|---|
| | **Total** | **% Dead** |
| **Control** | 111 | 0 |
| **DHEA** | 166 | 47.5 |
| **CoA 5 mM** | 30 | 0 |
| **CoA 5 mM + DHEA** | 32 | 12.5 |

Fra- Fragmentation; C3P- Caspase-3 Positive